Precision & Performance Conference 2025, Cranfield University, UK, 17th- 20th November 2025

Uncertainty analysis of positioning deviations of machine tools' linear axes: A foundation for uncertainty evaluation of volumetric deviations

Morteza Dashtizadeh[1], Andrew Longstaff[1], Simon Fletcher[1]

[1] *Centre for precision technologies, University of Huddersfield, UK*

M.dashtizadeh2@hud.ac.uk

Abstract

This paper presents an uncertainty assessment of positioning deviations at multiple target positions of a machine tool's linear axes, measured with a Renishaw XM-60 laser system over one year. The analysis, based on GUM and ISO/TR 230-9 and ISO 230-2, Annex A, forms a foundation for evaluating volumetric deviation uncertainties across all error motions. Seven main contributors were quantified, with thermal expansion coefficient, temperature, and axis repeatability accounting for the average of 40%, 20%, and 19% of the total expanded uncertainty, respectively. Improved thermal control and compensation timing could reduce uncertainty by more than 50%. The methodology is general and can be applied to any machine tool axis, measuring system, and environmental condition.

Keywords: Machine tools metrology, Positioning deviations, Uncertainty analysis, Volumetric errors

1. Introduction

Measurement uncertainty for machine tool tests has long been a challenge in industrial environments. This issue remains persistent in workshop conditions when a non-conformity takes place on a machined part. Knapp [1] addressed the measurement uncertainty of machine tools tests. ISO/TR 230-9 [2] presents the basic equations required to estimate the uncertainty of positioning errors along with a list of uncertainty contributors. From the perspective of acceptance positioning tests, ISO 230-2 [3] specifies how to express expanded uncertainty for different positioning error terms defined in this standard including terms M, A, E, U, and R. Donmez et al. [4] and Okafor and Ertekin [5] used Homogeneous Transformation Matrices (HTM) to mathematically model error vectors of 2-axis and 3-axis machine tools, respectively. Vahebi and Arezoo [6] used measured error motions to compute the volumetric errors of a gantry milling machine using HTM equations. Fesperman et al. [7] also predicted the tool path of several machine tools with different kinematic chains using HTM methodology. Dashtizadeh et al. [8] statistically studied the volumetric errors of machining centres conforming to ISO 10791 tolerances, also using HTM equations.

Technically, utilising HTM is a common method to derive volumetric deviations across the working volume of a machine tool based on rigid body theory. To obtain that, all deviations (three linear and three angular) at each target position are measured and incorporated into the HTM mathematical model. To address the uncertainty of the volumetric deviations, the uncertainty of all six error motions of all axes must be estimated at each target position. Therefore and in contrast to the method presented in ISO 230-2, Annex A, this paper focuses on the uncertainty of deviations at the target positions, some of which have non-linear correlations, rather than over the full axis travel. The deviations as well as their uncertainties studied in this research can be used to propagate the volumetric uncertainty within the machine's working volume.

For this study, all experiments were conducted on a 3-axis vertical machining centre (VMC) shown in **Figure 1** using Renishaw XM-60 laser system. The three axes of the Cincinnati Arrow 500 VMC were each approximately 500 mm in length.

Figure 1. Test setup to measure error motions of Y-axis on the Cincinnati Arrow 500 VMC by the Renishaw XM-60

2. Uncertainty contributors to positioning deviations

With reference to ISO/TR 230-9 [2], seven main influeincing parameters were identified as uncertainty contributors to positioning deviations. These contributors are listed as 'measuring instrument', 'alignment of the laser interferometer to the guideway/linear scale', 'ambient temperature', 'expansion coefficient of the linear scale', 'environmental variation', 'repeatability of Abbe offset', and 'repeatability of the machine axis'. Clause 3 numerically presents the expanded uncertainty of the positioning deviations associated with these contributors.

3. Quantifying expanded uncertainty due to each contributor

3.1. Expanded uncertainty due to the measuring instrument

The general form of the expanded uncertainty associated with the laser interferometer is $U_{Device} = k \times \frac{R_{Device} \times L}{1000 \times 2\sqrt{3}}$. **Figure 2** shows the expanded uncertainty of the positioning deviations at different target positions for various device errors over an axis length of 500 mm. R_{Device} for the Renishaw XM-60 is ±0.5 ppm.

3.2. Expanded uncertainty due to misalignment during the test

The equation of $U_{Misalignment} = k \times \frac{1000 \times R_{Misalignment}^2}{2\sqrt{3} \times 2L}$ gives the expanded uncertainty due to misalignment. **Figure 3** presents the expanded uncertainty due to this contributor for various misalignment ranges over axis lengths up to 500 mm. The maximum $R_{Misalignment}$ by which it is possible to conduct a positioning test with the Renishaw XM-60 over the axis of 500 mm is 1 mm.

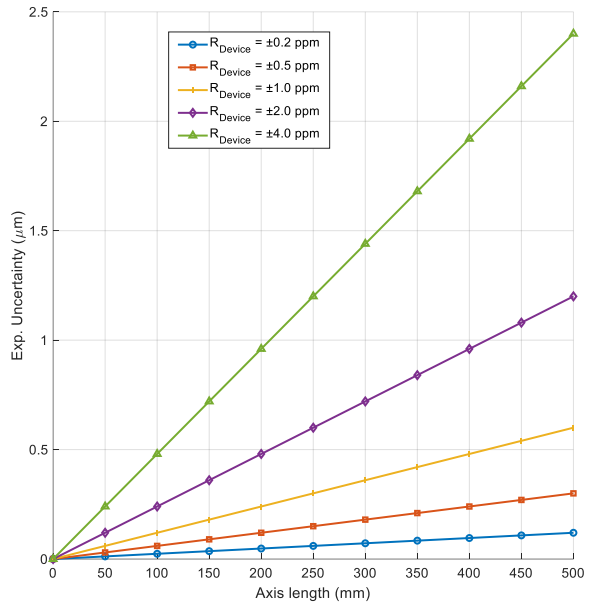

Figure 2. Expanded uncertainty of positioning deviations at different axis positions (lengths) up to 500 mm due to the measuring device with different error ranges, R_{Device} from ±0.2 ppm to ±4 ppm

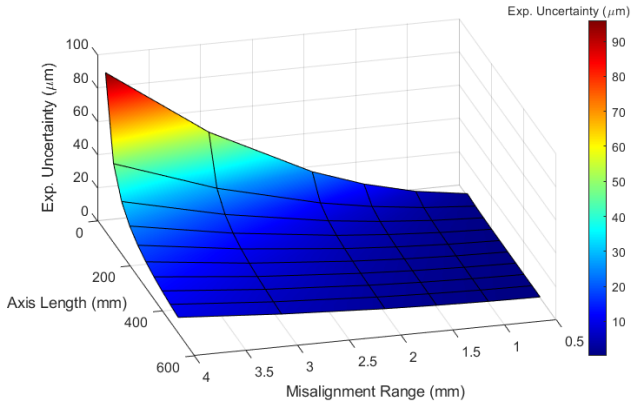

Figure 3. Expanded uncertainty of positioning deviations due to misalignment ranging from 0.5 mm to 4 mm for an axis length of 500 mm

3.3. Expanded uncertainty due to ambient temperature

The equation of $U_{\Delta l_\theta} = k \times \frac{\alpha \cdot l_{\theta 20} \cdot R_\theta}{2\sqrt{3}} \times 1000$ provides the expanded uncertainty of positioning deviation due to ambient temperature measurements. **Figure 4** illustrates the expanded uncertainty due to temperature measurement error, R_θ, for values ranging from 0.1 °C to 4 °C for glass linear scales installed on the Cincinnati VMC with $\alpha = 8.5\ \mu m/m°C$, and an axis length of up to 500 mm.

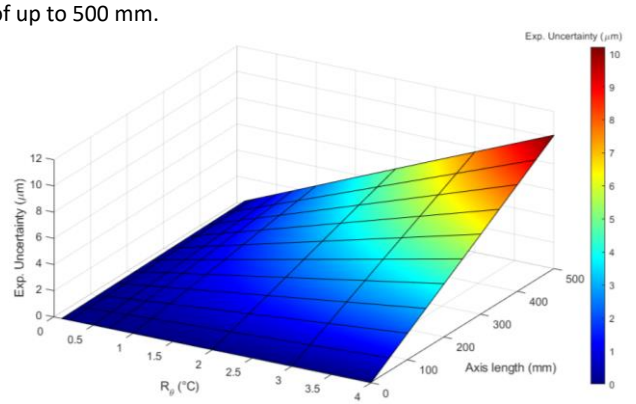

Figure 4. Expanded uncertainty of positioning deviations due to temperature measurement accuracy ranging from 0.1 °C to 4 °C over different length of axis up to 500 mm

According to the manufacturer's specification, the Renishaw material temperature sensor has an accuracy of ±0.1 °C. Therefore, in the best-case scenario, with this sensor located adjacent to the linear scale, $R_\theta = 0.2$ °C is achievable. However, during testing on the Cincinnati, this sensor was mounted on the machine's table. Assuming the table surface temperature may differ by ±0.5 °C from the actual scale temperature, a practical R_θ value of approximately 1.2 °C can be expected under workshop conditions.

3.4. Expanded uncertainty due to expansion coefficient of the material

The equation $U_{\Delta l_\alpha} = k \times \frac{\Delta\theta \cdot l_{\theta 20} \cdot R_\alpha}{2\sqrt{3}} \times 1000$ gives the expanded uncertainty of positioning deviations for different lengths due to the uncertainty of thermal expansion coefficient assuming a rectangular distribution for these expansion errors. ISO/TR 230-9 suggests considering R_α equal to the minimum range of 10% of the nominal value of the thermal expansion coefficient but not smaller than 2 µm/m°C. For the Cincinnati VMC with glass scale of nominal thermal expansion coefficient 8.5 µm/m°C, R_α is assumed to be 2 µm/m°C. Based on this assumption, **Figure 5** shows the expanded uncertainty of the positioning error at different temperatures ranging from 5 °C to 35 °C.

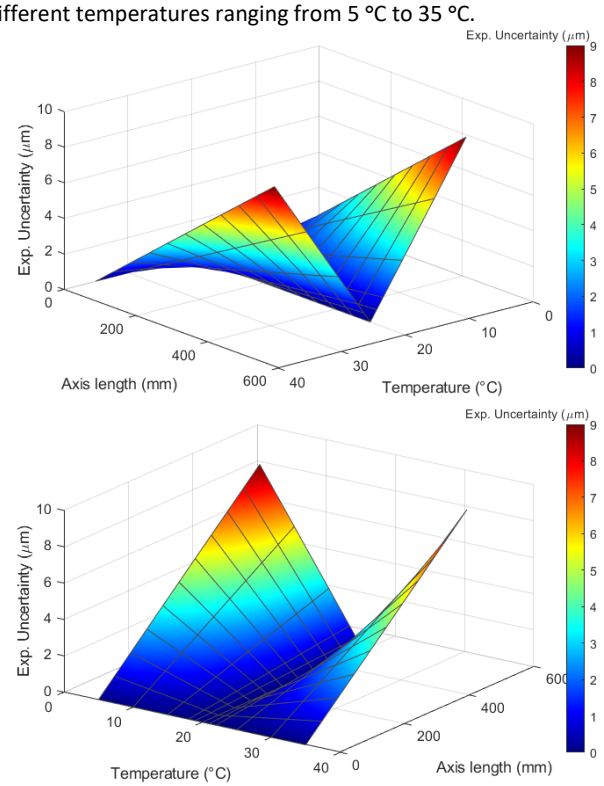

Figure 5. Expanded uncertainty of positioning deviations due to expansion coefficient accuracy of 2.0 µm/m°C over axis lengths of up to 500 mm from two viewpoints

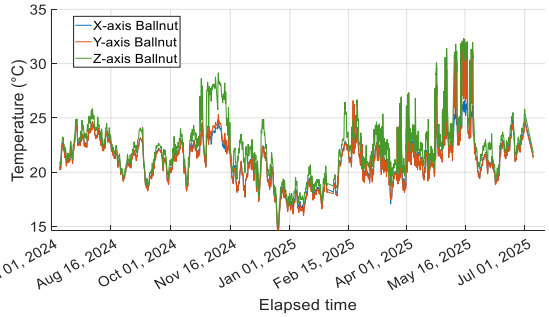

Figure 6. Temperature of the Cincinnati linear axes over one year

Figure 6 shows the monitored temperature of the three axes of the Cincinnati VMC throughout an entire year, representing their usual working conditions during different seasons. The maximum temperature difference recorded from the standard temperature

of 20 °C, $\Delta\theta$, is observed as 12 °C. Therefore, this maximum temperature difference is used for uncertainty estimation due to the thermal expansion coefficient error of the linear axes.

3.5. Expanded uncertainty due to environmental variation errors (EVE)

Although ISO/TR 230-9 suggests capturing data at the extreme position of the axis, this test was carried out at all target positions shown in **Figure 7**. The expanded uncertainty due to EVE is obtained using equation $U_{EVE} = k \times \frac{\Delta e_{YY_{EVE}}}{2\sqrt{3}}$ for each target position. This analysis indicates that the largest variations occurred at a position other than the extreme Y-axis position. However, it should be noted that over the period of 10 minutes of testing at each target position, the positioning variations never exceeded 0.001 mm

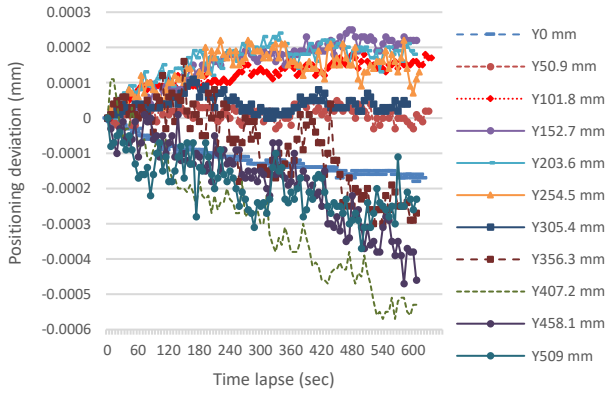

Figure 7. Positioning EVE deviations at different target positions of the Y-axis over 10 minutes period

3.6. Expanded uncertainty due to Abbe offset

Changes in the laser system setup result in different positioning deviations at each target positions due to variations in Abbe-offset lengths.

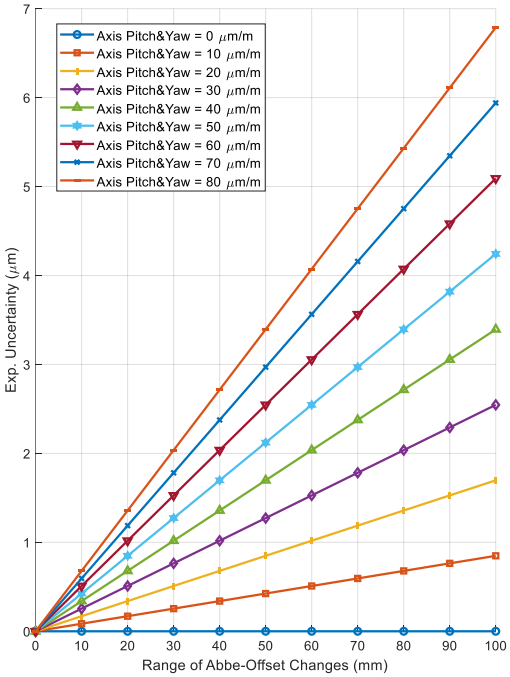

Figure 8. Expanded uncertainty of positioning deviations due to changes in Abbe-offset lengths in different positioning tests

The equation $U_{Abbe} = k \times \frac{\sqrt{(eCY \times X_{Abbe\_Y})^2 + (eAY \times Z_{Abbe\_Y})^2}}{2\sqrt{3} \times 1000}$ gives the expanded uncertainty of the positioning deviation due to this change. **Figure 8** shows the expanded uncertainty of the positioning deviations for different laser system setups with Abbe offset from 0 mm to 100 mm and for different angular errors of pitch and yaw ranging from 0 µm/m to 80 µm/m. According to ISO/TR 230-9, it is assumed that the laser system on the Cincinnati Y-axis can be setup with 50 mm Abbe offset changes along both X- and Z-axes for different positioning tests.

3.7. Expanded uncertainty due to axis repeatability

Besides the above contributors, the machine axis itself is another contributor to the positioning deviation uncertainty. From a 5-bidirectional run positioning test on the Y-axis of the Cincinnati VMC as demonstrated in **Figure 9**, the positioning repeatability is evaluated as ±2 standard deviations from the measured deviations at each target position.

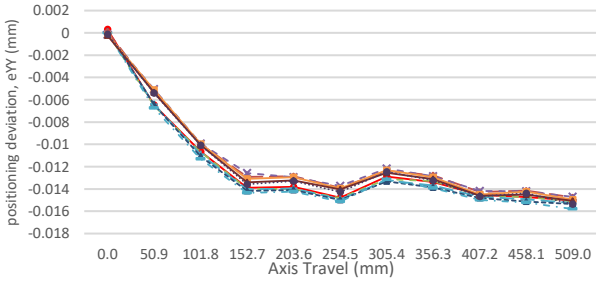

Figure 9. Positioning deviations of the Cincinnati Y-axis, eYY, over a 5-bidirectional run test measured by the Renishaw XM-60 laser system

4. Combined expanded uncertainty of positioning deviation

Using the equations and values presented in clause 3.1 to 3.7 and combining them according to GUM [9] computes the expanded uncertainty at each target position. **Figure 10** presents the positioning deviations of the Y-axis alongside their associated expanded uncertainties with the coverage factor k=2.

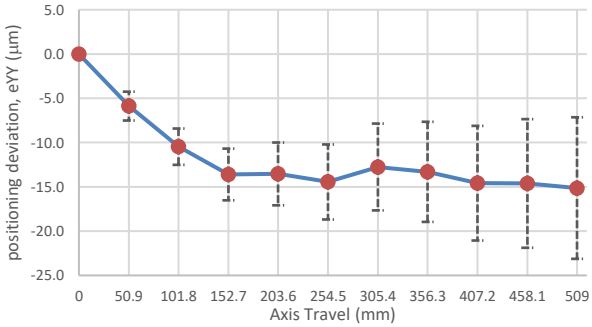

Figure 10. Positioning deviations of the Y-axis, eYY, along with the expanded uncertainty with k=2

5. Contribution of each uncertainty source

Figure 11 is a pie chart showing the contribution of each uncertainty source to the overall expanded uncertainty, both in µm and as a percentage of the expanded uncertainty at the extreme target position of 509 mm.

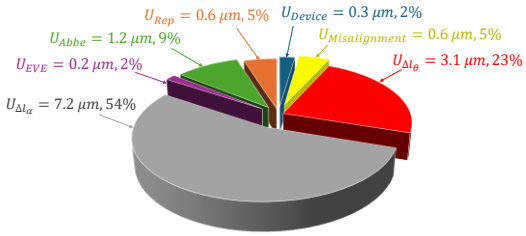

Figure 11. Contribution to expanded uncertainty of 8 µm for positioning deviation at extreme position of Y=509 mm

This chart highlights which contributor has the greatest impact on the final uncertainty. The uncertainty associated with the thermal expansion coefficient has an absolute expanded uncertainty of 7.2 µm, obtained assuming R_α = 2 µm/m°C and

$\Delta\theta$ = 12 °C. This represents 54% of the total expanded uncertainty of 8 µm. In other words, eliminating the effect of this contributor would reduce the overall expanded uncertainty at Y=509 mm by 54%. The second most significant uncertainty contributor is the length changes due to the temperature uncertainty, $U_{\Delta l_\theta}$. Together, these two contributors account for more than 75% of the uncertainty.

Similar pie charts can be generated for each of the other 10 target positions along the Y-axis. The percentage contributions vary depending on how each uncertainty source influences the positioning deviation. To investigate this, a cumulative plot showing the effect of all contributors on the total expanded uncertainty across all target positions of the Y-axis can be generated. **Figure 12** shows in µm the contribution of each uncertainty source at each Y-axis target position.

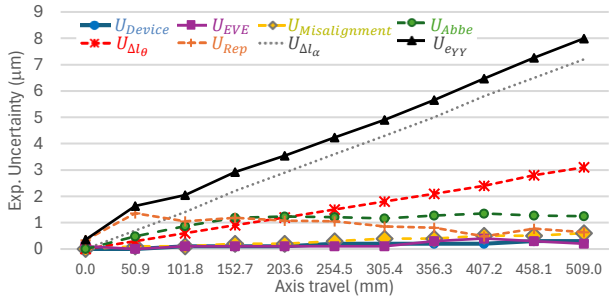

Figure 12. Expanded uncertainty of the Y-axis positioning deviations, U_{eYY}, with k=2 at each target positions with contribution of each uncertainty source

6. Average absolute and percentage contribution of each uncertainty source over the axis

Figure 13 and **Figure 14** present the average absolute and percentage contributions of each uncertainty contributor, respectively for all three linear axes of the Cincinnati VMC. The three most significant contributors are 'thermal expansion coefficient', 'material temperature', and 'machine axis repeatability'. According to **Figure 13**, $\overline{U}_{\Delta l_\alpha}$ contributes on average 3.6 µm to the average of absolute expanded uncertainty of the Y-axis, $\overline{U}_{eYY}$ equals 4.3 µm. On the X-axis and Z-axis, the average contribution of $\overline{U}_{\Delta l_\alpha}$ is 2.0 µm and 3.3 µm, respectively, out of the total average absolute expanded uncertainty of 2.8 µm and 3.8 µm.

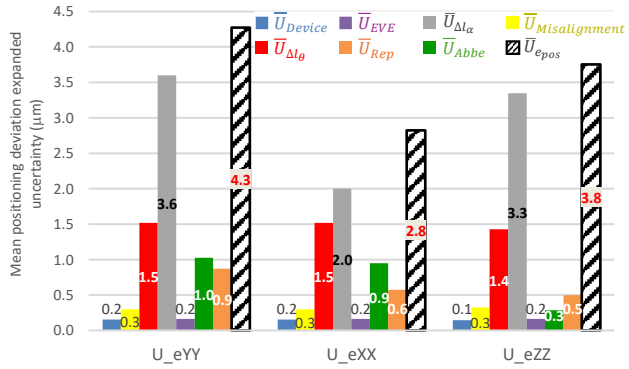

Figure 13. Average absolute contribution of each contributor to expanded uncertainty of positioning deviations with k=2 for all axes

Figure 14 shows that the average influence of the major three contributors of $U_{\Delta l_\alpha}$, $U_{\Delta l_\theta}$, and U_{Rep} for all target positions of the Y-axis are 40%, 17%, and 21%, respectively. On the X-axis, the relative percentage of $U_{\Delta l_\alpha}$ is 32%, the relative percentage of $U_{\Delta l_\theta}$ is 24% and the relative percentage of U_{Rep} is 19%. On the Z-axis, they are 48%, 21% and 16%, respectively. The cumulative contribution of these three contributors, averaged over all target positions, is therefore 74% for the X-axis, 78% for the Y-axis, and 85% for the Z-axis.

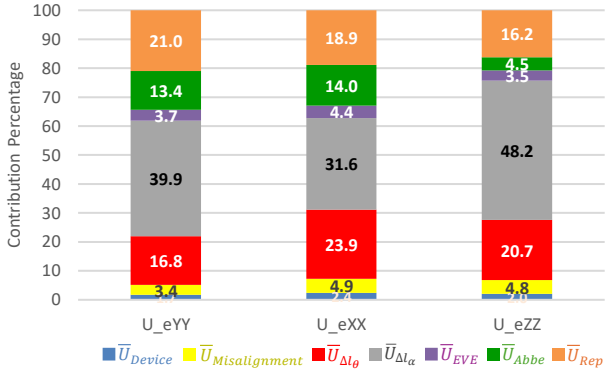

Figure 14. Average percentage contribution of each contributor to expanded uncertainty of positioning deviations for all axes

7. Summary and conclusion

This paper presented an uncertainty analysis of positioning deviations providing a suitable foundation for uncertainty assessment of volumetric deviations. The thermal expansion coefficient is the largest contributor in this study to the overall expanded uncertainty. By monitoring ambient temperature, the timing of axis compensation can be optimised for different cold and warm seasons, reducing uncertainty by more than 50%.

Acknowledgement

The authors would like to acknowledge the UK's Engineering and Physical Sciences Research Council (EPSRC) funding of The Future Advanced Metrology Hub for Sustainable Manufacturing (Ref. EP/Z53285X/1) and UKRI's funding of the Advanced Machinery & Productivity Initiative (Ref. 84646). The authors also extend their gratitude to Andrew Bell and Ashley Cusack for their valuable contribution to the experiments and temperature data processing.

References

[1] W. Knapp, "Measurement Uncertainty and Machine Tool Testing,"*CIRP Annals,* vol. 51, no. 1, pp. 459-462, 2002, doi: 10.1016/s0007-8506(07)61560-1.

[2] *ISO/TR 230-9:2005, Test code for machine tools — Part 9: Estimation of measurement uncertainty for machine tool tests according to series ISO 230, basic equations*

[3] *ISO 230-2:2014, Test code for machine tools — Part 2: Determination of accuracy and repeatability of positioning of numerically controlled axes*

[4] M. A. Donmez, D. S. Blomquist, R. J. Hocken, C. R. Liu, and M. M. Barash, "A general methodology for machine tool accuracy enhancement by error compensation," *Precision Engineering,* vol. 8, no. 4, pp. 187-196, 1986/10/01/ 1986, doi: https://doi.org/10.1016/0141-6359(86)90059-0.

[5] A. C. Okafor and Y. M. Ertekin, "Derivation of machine tool error models and error compensation procedure for three axes vertical machining center using rigid body kinematics," *International journal of machine tools & manufacture,* vol. 40, no. 8, pp. 1199-1213, 2000, doi: 10.1016/S0890-6955(99)00105-4.

[6] M. Vahebi and B. Arezoo, "Accuracy improvement of volumetric error modeling in CNC machine tools," *The International Journal of Advanced Manufacturing Technology,* vol. 95, no. 5-8, pp. 2243-2257, 2017, doi: 10.1007/s00170-017-1294-x.

[7] R. R. Fesperman, S. P. Moylan, G. W. Vogl, and M. A. Donmez, "Reconfigurable data driven virtual machine tool: Geometric error modeling and evaluation," *CIRP Journal of Manufacturing Science and Technology,* vol. 10, pp. 120-130, 2015, doi: 10.1016/j.cirpj.2015.03.001.

[8] M. Dashtizadeh, A. Longstaff, and S. Fletcher, "Estimation of volumetric errors of a machining centre fabricated with conformance to geometric tolerances of ISO 10791 series," presented at the Laser Metrology and Machine Performance, Edinburgh, Uk, 2023.

[9] *JCGM 100:2008, Evaluation of measurement data - Guide to the expression of uncertainty in measurement (GUM)*